journal of the mechanical behavior of biomedical materials 135 (2022) 105451

Contents lists available at ScienceDirect

Journal of the Mechanical Behavior of Biomedical Materials

journal homepage: www.elsevier.com/locate/jmbbm

Stability of fatigued and aged ZTA compared to 3Y-TZP and Al_2O_3 ceramic systems

Ernesto B. Benalcázar Jalkh [a,f,*], Edmara T.P. Bergamo [a,f], Tiago M.B. Campos [a], Everardo N. S. de Araújo-Júnior [a], Adolfo C.O. Lopes [a], Sérgio M. Tebcherani [b], Satoshi Yamaguchi [c], Luis A. Genova [d], Petra C. Gierthmuehlen [e], Lukasz Witek [f,g], Paulo G. Coelho [h], Estevam A. Bonfante [a]

[a] Department of Prosthodontics and Periodontology, University of São Paulo, Bauru School of Dentistry, Bauru, SP, Brazil
[b] Federal University of Technology, Paraná, Department of Production Engineering, Av. Monteiro Lobato km 04, 84016-210, Ponta Grossa, PR, Brazil
[c] Department of Biomaterials Science, Osaka University Graduate School of Dentistry, Suita, Osaka, Japan
[d] Nuclear and Energy Research Institute, IPEN, SP, Brazil
[e] Department of Prosthodontics, Medical Faculty and University Hospital Düsseldorf, Heinrich-Heine-University, Düsseldorf, Germany
[f] Department of Biomaterials and Biomimetics, New York University College of Dentistry, New York, NY, USA
[g] Department of Biomedical Engineering, NYU Tandon School of Engineering, New York University, Brooklyn, NY, USA
[h] Department of Surgery, University of Miami Miller School of Medicine, Miami, FL, USA

ARTICLE INFO

Keywords:
Zirconia
Alumina
Fatigue
Reliability
Microstructure
Aging

ABSTRACT

To evaluate the effect of fatigue and aging on the crystalline content and reliability of a zirconia-toughened-alumina (ZTA) composite compared to its individual counterpart materials (3Y-TZP and Al_2O_3).

Thirty-six disc-shaped specimens per group were obtained to comply with ISO 6872:2015. Crystalline content, microstructure and reliability of experimental groups were evaluated in four stages: 1) immediate; 2) aged; 3) fatigued; 4) aged + fatigue. Aging was performed in autoclave and Step-Stress-Accelerated-Life-Testing (SSALT) was performed using three stress profiles. Weibull statistics were used to determine Weibull parameters and life-expectancy. A significant increase in monoclinic phase in 3Y-TZP was observed after aging (19.31%), fatigue (17.88%) and aging + fatigue (55.81%), while ZTA evidenced minimal variation among all conditions (<5.69%). 3Y-TZP presented higher reliability than ZTA at 300 and 500 MPa, and ZTA outperformed Al_2O_3 at the same stress missions. None of the ceramics yielded acceptable reliability at 800 MPa. A higher characteristic strength was observed for 3Y-TZP, followed by ZTA and Al_2O_3. While after aging ZTA and Al_2O_3 remained stable, 3Y-TZP exhibited a significant increase in the characteristic stress.

Aging did not affect the reliability of ZTA and Al_2O_3. 3Y-TZP demonstrated an increase in monoclinic content and characteristic strength after aging.

1. Introduction

Among polycrystalline ceramics, zirconia has been broadly used in the biomedical field because of its highlighted mechanical properties and biocompatibility (Garvie et al., 1975). The first-generation dental zirconia, yttria-stabilized tetragonal zirconia polycrystals (3Y-TZP), is characterized by the stress mediated phase transformation from the metastable tetragonal phase to the monoclinic phase (t-m), where the volume increase associated with phase transformation is able to hinder crack propagation in the core (phenomenon known as transformation toughening). However, its high opacity makes it an interesting alternative only to overcome the esthetic drawbacks of metallic infrastructures, still requiring the porcelain veneering to achieve esthetics (Jung et al., 2008; Walton, 2013). It is noteworthy that along with the

Abbreviations: ZTA, zirconia-toughened-alumina; Y-TZP, yttria-stabilized tetragonal zirconia polycrystals; LTD, low temperature degradation; FDP, fixed dental prostheses.

* Corresponding author. Dept. of Prosthodontics and Periodontology, University of Sao Paulo, Bauru School of Dentistry, Al. Otávio Pinheiro Brisola 9-75, Bauru, SP, Brazil.

E-mail address: ernestobenalcazarj@gmail.com (E.B. Benalcázar Jalkh).

https://doi.org/10.1016/j.jmbbm.2022.105451
Received 20 June 2022; Received in revised form 31 August 2022; Accepted 2 September 2022
Available online 13 September 2022

remarkable mechanical properties of 3Y-TZP, the improvements in Computer-Aided Design and Computer-Aided Manufacture (CAD/CAM) technology, have provided faster and less expensive fabrication procedures for 3Y-TZP-based reconstructions (Joda et al., 2017). As a consequence, a wide clinical application of 3Y-TZP ceramics has been observed aiming not only to overcome the esthetic limitations of metallic frameworks, but also to increase the efficiency of prosthodontic treatments.

Systematic reviews evaluating the clinical performance of 3Y-TZP based restorations compared to its metal ceramics counterparts have reported high survival rates for tooth-supported (Sailer, Makarov et al. 2015, 2016) and implant-supported (Pjetursson et al., 2018) single crowns. Nonetheless, when indicated for long span rehabilitations, including partial and full-arch fixed dental prostheses (FDP), porcelain-veneered 3Y-TZP have shown inferior survival rates when compared to metal ceramics, irrespective of support (teeth or implants) (Pjetursson et al., 2017; Sailer, Strasding et al., 2018; Pjetursson et al., 2022). The higher risk for chipping of the veneering porcelain observed in clinical studies, as well as for framework fractures, have led to the assumption that conventionally veneered zirconia should not be considered as a first-choice system for FDPs (Sailer, Strasding et al., 2018; Pjetursson et al., 2022).

Aiming to eliminate the veneering ceramic interface and to obtain materials with greater structural integrity, translucent 3Y-TZP systems have been developed for monolithic (full-contour restoration) applications, named second-generation zirconia (Zhang and Lawn, 2017). However, the direct contact of 3Y-TZP to the oral environment raises concerns about potential adverse effects of its susceptibility to low temperature degradation (LTD) (Chevalier et al., 1999; Chevalier, 2006; Piconi et al., 2006; Chevalier, Gremillard et al., 2007). LTD is known by the spontaneous and progressive t-m phase transformation, resulting in volumetric grain alterations, which may increase the surface roughness (Chevalier, Grandjean et al., 2009), induce micro cracking, and eventually compromise 3Y-TZP mechanical (Chevalier and Gremillard, 2009, Chevalier, Grandjean et al., 2009; Sailer, Balmer et al., 2018) and optical (Kim and Kim, 2018) properties. Hence, LTD consequences on the microstructure integrity may influence the reliability of prosthetic treatments in the long-term (Kim, Han et al., 2009).

In light of the well documented limitations of 3Y-TZP systems currently used in dentistry, polycrystalline ceramic composites of zirconia and alumina have been proposed in the literature as a substitute for metallic and 3Y-TZP infrastructures (Benalcazar Jalkh et al., 2020b). Zirconia toughened alumina (ZTA), a ceramic composite comprised by a primary phase of alumina (Al_2O_3) and a secondary phase of 3Y-TZP (Kurtz et al., 2014), has been used in the orthopedic field since 2000 to overcome the detrimental hydrothermal instability of 3Y-TZP systems (Chevalier et al., 2000; Chevalier, Gremillard et al., 2009). The rationale behind ZTA applications relies on the combination of the best properties of both materials. While 3Y-TZP provides its highlighted mechanical properties due to the transformation toughening effect, Al_2O_3 provides a hard matrix that allows the stabilization of zirconia's tetragonal phase within the composite (Chevalier and Gremillard, 2009). The advantageous features of ZTA composites have led to a wide application in the orthopedic field for the manufacture of ceramic-on-ceramic prostheses for total hip replacement, where promising in-vitro results (Perrichon et al., 2017; Al-Hajjar et al., 2019) have been reported with a survival rate of up to 99% of femoral head protheses after 10 years (Howard et al., 2017).

Recent dental-based evidence have indicated high hydrothermal stability for ZTA composites comprised by 70% Al_2O_3 and 30% 3Y-TZP, where microstructure, crystalline content, optical and mechanical properties remained stable after aging, as well as comparable to those of 3Y-TZP systems (Benalcazar Jalkh et al., 2020b), which would allow its indication as framework materials for single crowns and fixed dental prostheses, according to ceramic systems standard requirements (ISO 6872). However, there is currently no evidence regarding ZTA behavior for dental applications when submitted to fatigue in a wet environment, as it occurs during the masticatory function. Thus, the present study sought to evaluate the fatigue behavior and changes in crystalline content of an experimental ZTA composite comprised by 30% 3Y-TZP and 70% Al_2O_3 before and after aging compared to its isolated counterpart materials. We hypothesized that the formulated ZTA composites would be resistant to the accelerated aging protocol and that the biaxial flexural fatigue strength would only be altered in the aged second-generation 3Y-TZP.

2. Materials and methods

2.1. Ceramic powders and samples preparation

In the present study, a ZTA composite comprised by high purity alumina (Al_2O_3, Baikalox Regular CR10, Baikowski, France) reinforced with a second-generation yttria-stabilized tetragonal zirconia polycrystals (3Y-TZP, Zpex, Tosoh Corporation, Japan) was synthesized and compared to its counterpart materials. The three synthesized and tested experimental groups were: 1) ZTA: Synthesized in a weight ratio of 70% Al_2O_3 and 30% 3Y-TZP, 2) 3Y-TZP; and 3) Al_2O_3. Composition of the ceramic powders used in the present study is summarized in Table 1.

The ZTA composite was synthesized as previously presented (Lopes et al., 2019, Benalcazar Jalkh, Bergamo et al. 2020). In brief, a suspension in ethanol containing alumina and zirconia powders (Al_2O_3-70% v ZrO_2-30%) was prepared and the blend was homogenized for 4 h in a friction mill with alumina spheres. The slurry was then dried in a rotary evaporator (801, Fisaton, São Paulo, Brazil) and the powders were granulated and sieved. Alumina powder was prepared in an ethanol suspension with 0.05% magnesium oxide and 1% of Polyvinyl Butyral binder (Sigma-Aldrich, St. Louis, Missouri, USA). The suspension was then processed until sieving.

3Y-TZP, Al_2O_3, and the experimental ZTA powders were uniaxially (1148 kgf/cm^2 for 30 s) and isostatically (2110Kgf/cm^2 for 30 s) pressed at room temperature to obtain disc shaped green body samples of all groups. Sintering of ceramic materials was performed for 1 h (Zyrcomat Furnance, Vita Zahnfabrink, Bad Säckingen, Germany) at 1550 °C for 3Y-TZP samples and at 1600 °C for ZTA and Al_2O_3. Both with heating and cooling rate of 4° per minute (Benalcazar Jalkh et al., 2020b). Polishing was performed in both disk surfaces using a semi-automatic polishing machine (Automet 2000; Buehler, Illinois, USA) with diamond disks and diamond suspensions of granulations up to 1 μm (ALLIED High-Tech Products, California, USA).

One hundred and eight disc-shaped specimens (n = 36/group) were prepared with final dimensions of 12 mm of diameter and 1 mm thickness as recommended by the ISO 6872:2015. Crystalline structure and surface imaging, as well as fatigue behavior were determined for all groups before and after autoclave accelerated artificial aging. Additionally, fractographic analysis of the fragments was performed.

2.2. Aging

Half of the samples of each group were subject to *in-vitro* low-temperature degradation (LTD) using autoclave (Vitale Class CD, Cristófoli, Campo Mourão, PR, Brasil) at 134 °C, under a 2.2 bar pressure, over a period of 20 consecutive hours. This protocol has been proven to effectively promote t-m phase transformation in 3Y-TZP-based materials, with a significant impact on its mechanical, optical and microstructural properties (Pereira et al., 2015; Lopes et al., 2019, Benalcazar Jalkh, Bergamo et al. 2020, Benalcazar Jalkh, Monteiro et al. 2020; Lopes et al., 2020).

2.3. X-ray diffraction (XRD)

The crystalline structure of all groups was analyzed by XRD (X'pert Power PANalytical, Netherlands) in four different stages: 1) immediate

Table 1
Composition of the second-generation 3Y-TZP and high purity Al_2O_3 powders.

3Y-TZP	Particle Size (nm)	Chemical Composition [wt.-%]							
		Y_2O_3 (mol%)		Al_2O_3	Na_2O		SiO_2	FeO_2O_3	HfO2
	40	3		≤0.1	≤0.04		≤0.02	≤0.01	<5.0
Al_2O_3	Particle Size (nm)	Crystal Structure		Chemical Analyses ICP (ppm)					
		Alpha	Gamma	Fe	Na	Si	Ca	K	Mg, Ti, Cr, Mn, Ni, Cu, Zn
	350	95%	5%	6	13	18	2	22	<1 each

(before aging); 2) after aging; 3) after fatigue; 4) after aging and fatigue. The scanning was performed on the Bragg θ-2θ geometry, equipped with a graphite monochromator and Cu Kα radiation (λ = 1.5406 Å), operating at a voltage of 40 kV and a current emission of 40 mA. The data were obtained in periods of 1.0 s and steps of 0.020 (2θ) of 20–70°. Baseline subtraction was performed in High-Score Plus Software (Malvern Panalytical Ltd, Westborough, Massachusetts, USA) for all XRD collected data. Monoclinic and tetragonal peaks were identified, and the area corresponding to peaks 28, 30 and 31.2° were recorded for monoclinic phase calculation.

ZTA and 3Y-TZP monoclinic phase percentage was calculated before and after aging through the formulas introduced by Toraya and Yoshimura (Toraya et al., 1984) as follows:

$$Xm = \frac{[Im(-111) + Im(111)]}{[Im(-111) + Im(111) + It(101)]}$$

$$\frac{Vm = 1.311 \times Xm}{1 + 0.311 \times Xm}$$

where I_m (−111) and I_m (111) represent the monoclinic peaks intensity (2θ = 28° and 2θ = 31.2°, respectively), I_t (101) indicates the intensity of the tetragonal peak (2θ = 30°), and V_m represents the monoclinic volumetric content.

2.4. Scanning electron microscope (SEM)

The micromorphology of the ceramic systems was analyzed by SEM (VEGA3-TESCAN, Brno-Kohoutovice, Czech Republic). SEM images were obtained at high vacuum, 5 kV accelerating voltage, 6–12 mm working distance, and magnifications up to 20,000×.

2.5. Step stress accelerated life testing (SSALT)

For SSALT, disc-shaped specimens were subjected to cyclic loads, with successively increasing stress levels, until its failure or suspension (Bonfante and Coelho, 2016). For testing, specimens were positioned on a piston-on-three-balls biaxial flexural strength test device in an all-electric precision fatigue system according to ISO 6872:2015 requirements (ElectroPuls E3000 Linear Torsion system, Instron, Norwood, MA, USA), and tested under fatigue at 15 Hz. SSALT was performed using three different load profiles (Fig. 1), where samples were distributed in a ratio of 3:2:1 to mild (n = 9), moderate (n = 6) and aggressive (n = 3) profiles respectively, as described in previous literature (Abernethy et al., 1983; Nelson, 2004; Bonfante and Coelho, 2016).

Profiles design was achieved through the biaxial flexural strength data of ZTA composites previously published by our group (Benalcazar Jalkh et al., 2020b; Lopes et al., 2020). Fatigue test was performed in humid, room temperature environment (~23 °C), with a sheet of polyethylene (0.1 mm thick) placed between the piston and the ceramic surface to reduce contact stress concentration, as recommended by ISO 6872:2015. Test was conducted until failure or suspension of the specimens.

Based upon the step-stress distribution of failures, the inverse power law life-stress relationship for damage accumulation and Weibull distribution (Zhao and Elsayed, 2005) model enabled the calculation and plot of the use level probability Weibull curves, represented by probability of failure versus number of cycles with the corresponding 95% two-sided confidence interval (CI) (Alta Pro 21; Reliasoft, Tucson, AZ). The use of level probability in Weibull analysis provides a beta (β) value that describes the failure rate behavior over time. When failure rate decreases over time (β < 1), it is commonly associated with early failures. When failure rates increase over time (β > 1), it is related to damage accumulation and fatigue, and when beta is equal to one (β = 1) it represents failures of a random cause. The reliability, which represents the probability of an item surviving a given number of cycles at a use level stress, was calculated for a mission of 50,000 cycles at 100, 300, 500 and 800 MPa (stress requirements described in ISO 6872:2015 for ceramic materials). For the mission reliability and β parameters calculated, the two-side 95% CI were calculated. As β was lower than 1 for a determined group, Weibull probability contour plot, represented by the Weibull modulus versus the characteristic strength, was calculated and plotted, where contours limits were determined by the calculation of the two-side 95% CI.

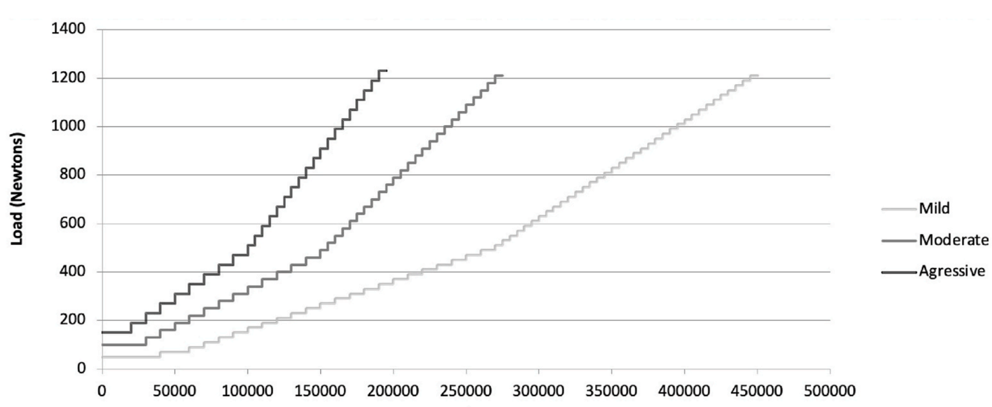

Fig. 1. Fatigue profiles designed for SSALT.

2.6. Fractographic analyses

The fractured specimens were examined with polarized light in Axio Zoom V16 Stereo Zoom Microscope (Carl Zeiss, Oberkochen, Germany) to assess fractographic evidence of the fracture origin and direction of propagation. The Z-stack imaging mode was used to merge images automatically taken on the z-plane into one figure with improved depth of focus (ZEN 2.3 PRO, Zeiss). Subsequently, SEM was used to confirm initial inspection and to document fractographic marks.

3. Results

X-ray diffraction data of all groups is presented in Fig. 2. XRD analyses allowed the identification of alpha (α) Alumina phase (Al_2O_3) and zirconia tetragonal (Z_T) and monoclinic (Z_M) phases (yttria-stabilized tetragonal zirconia polycrystals, 3Y-TZP). After background determination, 3Y-TZP and Al_2O_3 peaks were found using High-Score Plus Software, and the area under the 28°, 30° and 31.2° peaks were calculated to determine the percentage of tetragonal and monoclinic phases, according to Toraya and Yoshimura model (Table 2).

Images obtained with scanning electron microscope (SEM) at 20,000 magnifications exhibited a dense and homogeneous microstructure, which demonstrate the successful experimental processing protocol proposed for all ceramics tested (Fig. 3). A homogeneous distribution of 3Y-TZP grains on the Al_2O_3 matrix can be observed in the ZTA composites micrographs. While large grains can be noted in pure Al_2O_3, reduced grains were observed in the microstructure of the ZTA composite. Few microstructural defects can be observed for all ceramics, which are considered intrinsic to material processing (Fig. 3).

The step stress derived use level probability Weibull curves are presented in Fig. 4 to illustrate the failure distribution of the samples as a

Table 2
Monoclinic phase percentage of 3Y-TZP and ZTA ceramic systems before and after aging, and fatigue testing.

Material	Aging/Fatigue testing	Monoclinic phase %
3Y-TZP	Immediate	7.09
	Immediate + SSALT	17.88
	Aged	19.31
	Aged + SSALT	55.81
ZTA	Immediate	<1
	Immediate + SSALT	1.18
	Aged	2.12
	Aged + SSALT	5.69

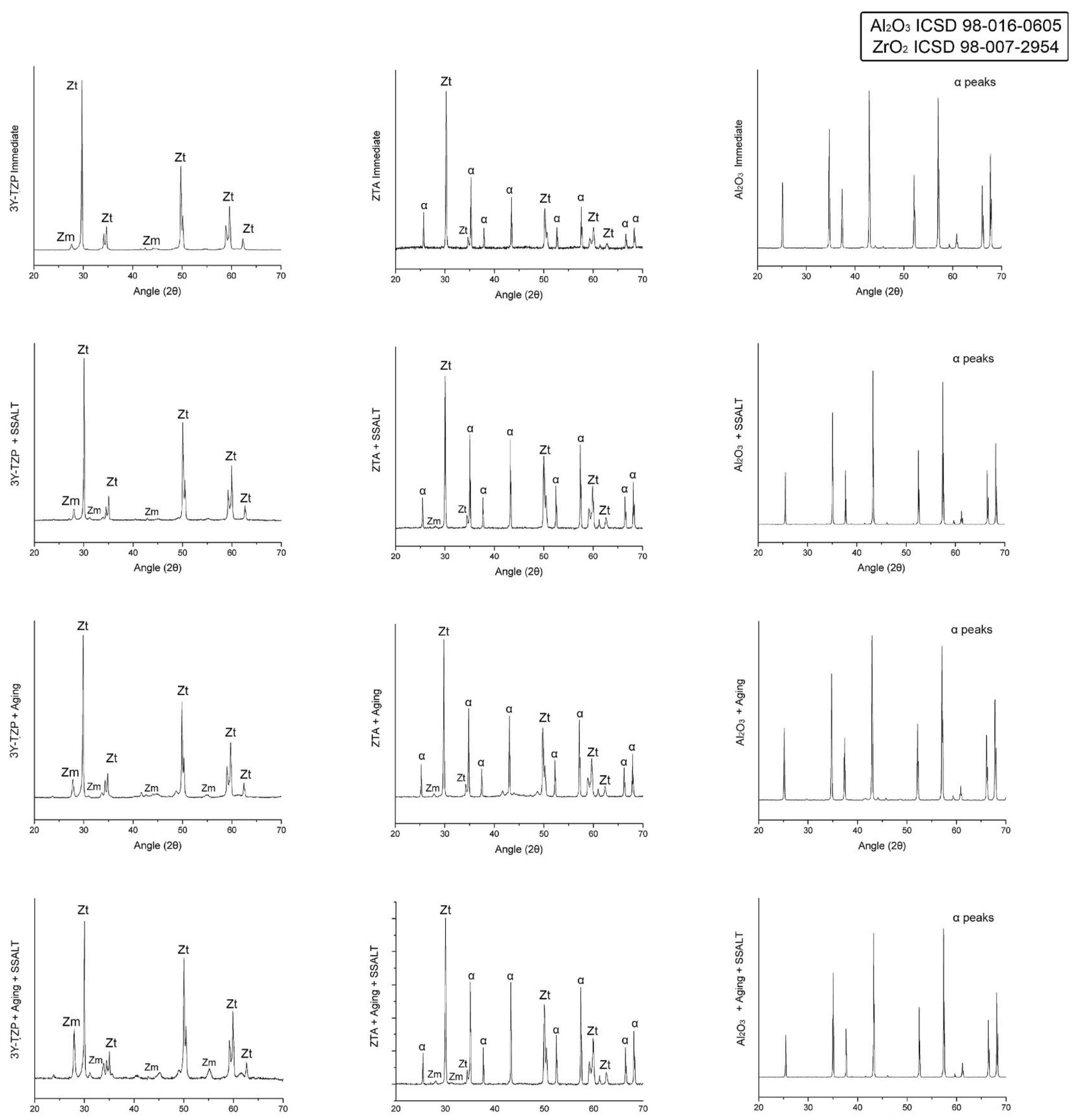

Fig. 2. XRD patterns of 3Y-TZP, ZTA and Al_2O_3 before fatigue (immediate), after aging, after fatigue, and after aging and fatigue testing.

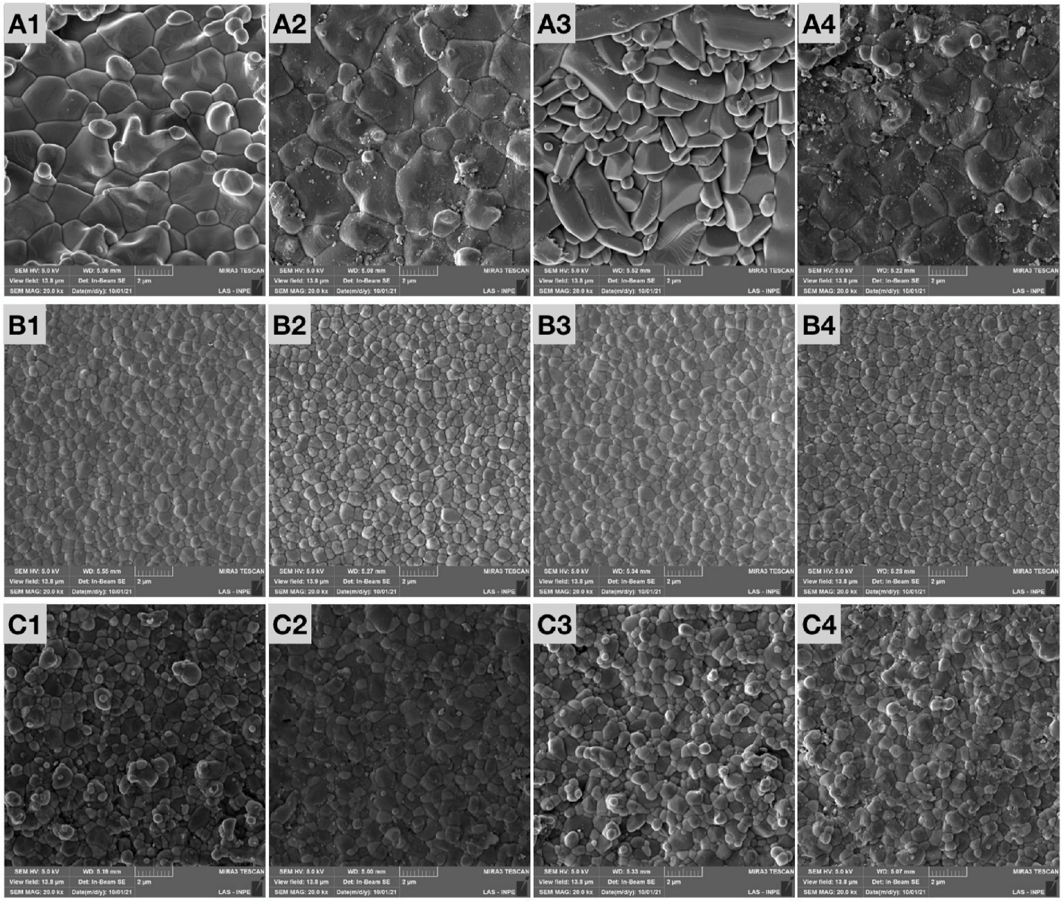

Fig. 3. SEM images of A) Al_2O_3, B) 3Y-TZP, and C) ZTA at 20,000×. Numbers indicate the condition of testing: 1) immediate, 2) immediate + SSALT, 3) aged in autoclave and 4) aged in autoclave + SSALT, respectively.

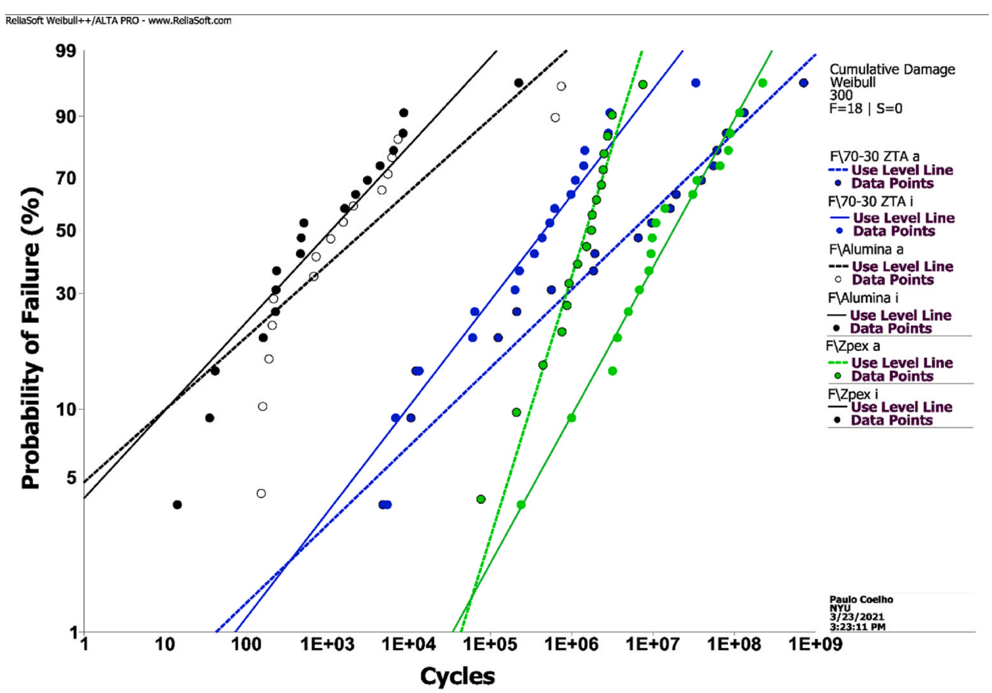

Fig. 4. Use level Weibull probability plot showing the probability of failure as a function of cycles and specimen failure distribution.

function of time. The beta (β) value obtained from the use level probability Weibull calculations was lower than one ($\beta < 1$) for all groups ($\beta = 0.35$–0.67), except for aged 3Y-TZP ($\beta = 1.19$); however, the lower bound of the confidence interval of aged 3Y-TZP was also lower than one, indicating that for all groups materials strength dictated the failure. The probability of survival for a mission of 50,000 cycles at relevant stresses (ISO 6872:2015) is summarized in Table 3. All ceramic materials presented a reliability close to 100% at 100 MPa, which is a stress value compatible with the indication of single crowns. The probability of survival of Al_2O_3 discs was significantly reduced, almost 0%, at a mission of 300 MPa. While immediate 3Y-TZP showed a significantly higher reliability than ZTA, aged 3Y-TZP and ZTA demonstrated no significant difference at a mission of 300 MPa, which is a stress value compatible with the indication of anterior fixed dental prostheses (FDPs). At 500 MPa, ISO requirements for posterior FDPs, the reliability Al_2O_3-based materials (including ZTA) dropped significantly, which discourage its indication for the manufacture of infrastructure of three or more units FDPs. Despite 3Y-TZP presented favorable reliability at 500 MPa, irrespective of aging, none of the ceramics tested in the present study yielded acceptable reliability at 800 MPa, which is compatible with the indication of FDPs with four or more units.

As per $\beta < 1$, the Weibull parameters were determined based on the stress at failure data. Weibull modulus, used as a measure that expresses the structural reliability of the material, and characteristic strength, which represents the stress at a failure probability of approximately 63.2% of all groups are summarized in Table 4. Weibull modulus of all groups demonstrated no significant difference, except for aged 3Y-TZP which showed significantly higher values than ZTA and Al_2O_3 in the aged condition. 3Y-TZP presented the highest values of characteristic strength, which significantly increased after aging, both significantly different from other ceramics. ZTA composite presented intermediate values of characteristic strength, with no significant difference after aging; however, both values were significantly higher when compared to pure Al_2O_3. Likewise, Al_2O_3 values of characteristic strength remained constant after aging (Fig. 5).

Fractographic analyses demonstrated similar fracture patterns for all ceramic systems. Characteristic fractographic marks, including hackle lines and compression curls, were used to suggest the origin of the fracture, in all the cases related to microstructural defects on the tensile side of the discs that propagated to the compression side of the specimens. Fig. 5 summarizes the micrographs of representative fractured discs of each material after fatigue testing.

Table 3
Probability of survival of all ceramic systems with the corresponding 95% CI for all groups.

		Immediate			Aged		
		ZTA	Al_2O_3	3Y-TZP	ZTA	Al_2O_3	3Y-TZP
100 MPa	Upper Bound	99	97	100	100	97	100
	Reliability	**97 Aa**	**92 Aa**	**100 Aa**	**99 Aa**	**92 Aa**	**100 Aa**
	Lower Bound	90	80	99	95	79	98
300 MPa	Upper Bound	89	14	1	95	32	100
	Reliability	**79 Ab**	**4 Ac**	**99 Aa**	**88 Aa**	**17 Ab**	**99 Aa**
	Lower Bound	63	0	94	74	6	94
500 MPa	Upper Bound	30	0	93	31	0	97
	Reliability	**16 Ab**	**0 Ac**	**86 Aa**	**17 Ab**	**0 Ac**	**91 Aa**
	Lower Bound	7	0	71	7	0	74
800 MPa	Upper Bound	0	0	4	0	0	29
	Reliability	**0 Aa**	**0 Aa**	**0 Aa**	**0 Ab**	**0 Ab**	**10 Ba**
	Lower Bound	0	0	0	0	0	2

Capital letters denote statistical differences between immediate and aged conditions. Non-capital letters denote statistical differences among experimental materials.

4. Discussion

During function, dental prostheses are subjected to repetitive lower-intensity stresses that lead to cumulative damage and slowly compromise the integrity of the restoration, eventually leading to failure at lower stress levels compared to its ultimate characteristic strength (Bonfante and Coelho, 2016). Such mechanisms seem critical in 3Y-TZP based restorative materials, where the metastability of the tetragonal phase may be affected by mechanical stress, humidity and body temperature(Kocjan et al., 2020; Cotic et al., 2021). Therefore, the present study aimed to evaluate the crystalline microstructure and the impact on reliability in non-aged controls, non-aged and fatigued, solely aged, and aged and fatigued ZTA experimental composite compared with its isolated counterpart materials. 3Y-TZP presented the highest values of characteristic strength, followed by ZTA composite and Al_2O_3, all significantly different. While aging did not affect the reliability of ZTA composite and Al_2O_3, 3Y-TZP demonstrated a significant increase in the characteristic strength after aging. The hypothesis that the experimental ZTA would be resistant to the accelerated aging protocol and that the biaxial flexural fatigue strength would only be altered in the aged second-generation 3Y-TZP was accepted.

The x-ray diffraction spectra and monoclinic phase percentage calculation in the present study confirm the greater stability of the tetragonal phase of ZTA composites formulated with 70% of Al_2O_3 and 30% of 3Y-TZP after aging (2.12%) and fatigue testing (5.69%), notably lower when compared to the isolated 3Y-TZP counterpart (after aging: 19.31% and fatigue testing: 55.81%). Previous findings concerning the effect of aging on ZTA composites using the same autoclave aging protocol used in the present study have also demonstrated a slight increase in monoclinic content for ZTA composites (up to 3.3%) which was significantly lower relative to 3Y-TZP (approximately 26.5%) (Benalcazar Jalkh et al., 2020b). Aging resistant materials are highly desirable in clinical practice to avoid the long-term consequences of hydrothermal instability, and ZTA stability might be explained by two mechanisms: 1) the interruption of the nucleation and growth mechanism of LTD, where the interconnectivity of 3Y-TZP grains is limited by the Al_2O_3 matrix; and 2) reduced transformation toughening in ZTA composites due to the reduced 3Y-TZP content in its composition (Chevalier and Gremillard, 2009). It is worthy to mention the effect of cyclic loading and the associated tensile stresses on increasing the monoclinic content, especially for 3Y-TZP before and after aging, where the findings demonstrate its susceptibility to the effects of LTD in combination with the transformation toughening induced by the mechanical stress produced by loading (Chevalier, Gremillard et al. 2007, 2009).

Second-generation 3Y-TZP was introduced as an alternative to first-generation 3Y-TZP for the manufacture of monolithic prostheses and the elimination of the veneering process due to improved optical properties, which has been achieved by reducing additive content and altering sintering protocols (Zhang and Lawn, 2017). In fact, such gain in translucency of second-generation 3Y-TZPs relies especially on the reduction of the Al_2O_3 content, the increase of the grain size, and reduction of defects and porosities of the surface to improve light transmittance (Tong et al., 2016), where the former factors have been reported to potentially increase the effects of hydrothermal aging of 3Y-TZP systems (Lucas et al., 2015). The laboratory simulation of hydrothermal degradation using autoclave has been effective in promoting zirconia tetragonal-to-monoclinic (t-m) phase transformation (Pereira

Table 4
β values and Weibull Parameters [Weibull modulus (*m*) and Characteristic strength (η)] with the corresponding 95% CI obtained for all groups.

	Immediate			Aged		
	ZTA	Al_2O_3	3Y-TZP	ZTA	Al_2O_3	3Y-TZP
Upper Bound	643.8	278.07	873.46	667.33	327.85	1038.31
Characteristic strength	595.37Ab	260.18Ac	828.75Aa	622.89Ab	298.14Ac	1001.22 Ba
Lower Bound	550.59	243.45	786.32	581.4	271.13	965.46
Upper Bound	7.08	8.35	10.36	8.01	6.18	15.85
Weibull Modulus	5.24Aa	6.18Aa	7.8Aa	5.95Ab	4.6Ab	11.61Aa
Lower Bound	3.88	4.57	5.87	4.42	3.42	8.51

Capital letters denote statistical differences between immediate and aged conditions. Non-capital letters denote statistical differences among experimental materials.

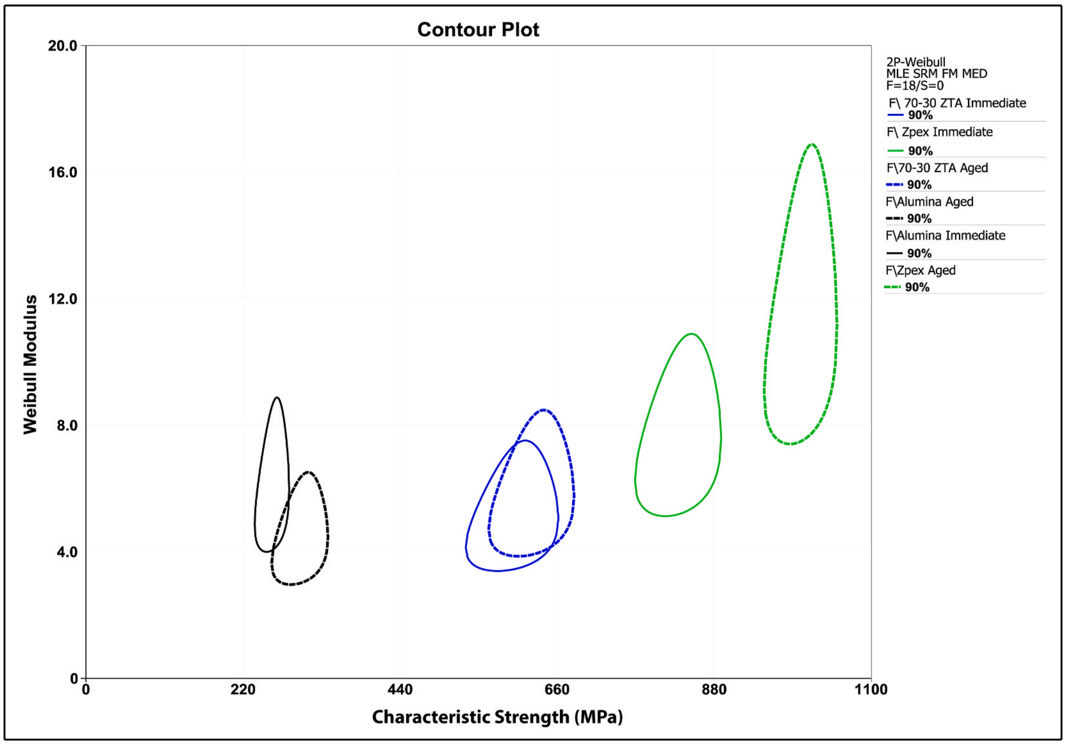

Fig. 5. Contour Plot of Characteristic strength (MPa) versus. Weibull Modulus (*m*). Dotted contour lines indicate aged samples.

et al., 2015) and is considered a standard method according to ISO 13356:2015 requirements (International-Standard-Organization, 2015). The ISO protocol, comprised by autoclave aging at 134 °C, 2.2 bar, for 5 h has been reported in orthopedic literature to be roughly equivalent to 2–4 years *in vivo* aging (37 °C) (Chevalier et al., 1999). However, recent evidence concerning the *in vivo* effects of LTD on 3Y-TZP systems have suggested that aging kinetics can be almost three times faster than the conventionally accepted *in vitro-in vivo* extrapolations (Kocjan et al., 2020). Furthermore, in a prospective clinical study with *ex vivo* monitoring of monolithic 3Y-TZP dental prostheses, Koenig et al. (2021) demonstrated that along with the effects of LTD, the tribological stresses generated in the occlusal surface of the prostheses produce surface crushing and grain pull-out, which suggest an underestimation of the aging process when characterization tests are limited to monoclinic phase quantification (Koenig et al., 2021). As mentioned above, the t-m transformation of the 3Y-TZP system herein studied generated from tensile stress of mechanical (19%) and chemical (17.88%) stimuli were similar, and the combination of both stimuli resulted in more than 55% monoclinic content. Such findings raise concerns regarding the clinical impact of hydrothermal-mechanical aging on second-generation 3Y-TZP as a monolithic reconstructive material and encourage the development/improvement of biomaterials, as well as laboratory methods that better simulate the complex characteristics of aging in the oral environment.

Based on failure distribution, fatigue analysis indicated that failure rate decreased over time and failure was chiefly dictated by materials strength rather than by damage accumulation (beta lower than one, $\beta < 1$, for all groups except for aged 3Y-TZP). Interestingly, the beta value higher than one ($\beta > 1$) for the aged second-generation 3Y-TZP can be associated with the extensive t-m transformation as a result of LTD simulation and mechanical loading. It has been well-defined that volumetric alterations caused by t-m transformation in 3Y-TZP systems produce residual compressive stress accumulation that can seal defects and limit crack propagation, increasing fracture toughness (Stump and Budiansky, 1989). However, when a critical tension accumulation is reached, there is a massive collapse of grains and an increase of defect population within the material that, consequently, reduces the flexural strength (Becher and Swain, 1992; Kim, Han et al., 2009; Prado et al., 2019). Therefore, the crystalline rearrangement and microstructural alteration of the 3Y-TZP grains after aging might explain not only the higher beta value, but also the increase in characteristic strength observed in aged 3Y-TZP (~160 MPa), where a longer LTD protocol would be necessary to induce the necessary critical tension for grains collapse and reduction on the fatigue strength of the system.

As mentioned above, 3Y-TZP presented higher characteristic strength when compared to ZTA composite and pure Al_2O_3. Based on previous biaxial flexural strength data, it was expected that fatigue would reduce the characteristic strength of all ceramic systems (Benalcazar Jalkh et al., 2020b). Although a decrease of approximately 200 MPa was observed for all immediate and aged groups after fatigue relative to the ultimate characteristic strength, a similar trend in statistical difference between groups was observed, with 3Y-TZP presenting the highest characteristic strength, followed by ZTA and Al_2O_3. Despite the higher amount of t-m transformation on the fatigued samples of 3Y-TZP, they have not reached the critical tension accumulation needed to produce a collapse on the grains and an increase in the defect population within the material, increasing the flexural fatigue strength. Up to a certain point, volumetric alterations caused by t-m transformation in 3Y-TZP systems lead to residual compressive stresses accumulation on the surface (area subjected to tensile stresses while fatigue testing) that limit the crack propagation, thus the higher transformability inherent to second-generation 3Y-TZP potentially resulted in a dense compressive layer on the surrounding grains, which limited crack propagation during testing and increased 3Y-TZP fatigue strength (Becher and Swain, 1992; Prado et al., 2019). In contrast, the Al_2O_3 matrix of ZTA composite limits the interconnectivity of 3Y-TZP grains, reducing not only LTD effects but also the benefits of transformation toughening. However, based on the current evidence that aging kinetics can be remarkably faster than extrapolations of *in vitro-in vivo* studies (Kocjan et al., 2020), aging resistant materials, such as ZTA composites, are highly desirable, especially when considering the range of stresses levels required for dental prostheses' applications.

Although ZTA composites have shown stability when only hydrothermally aged (Benalcazar Jalkh et al., 2020b), the literature has shown that orthopedic prostheses made of ZTA, retrieved in the short term (20 months), have shown up to 50% phase transformation (Rondinella et al., 2018). This finding suggests that along with low temperature degradation, the physiological loading of ZTA may produce a significant increase in phase transformation. However, the ZTA composite developed in the current study, subjected to both artificial hydrothermal aging and/or fatigue testing has shown high stability, with a relatively low phase transformation (<5.69%) when submitted to mechanical and hydrothermal stimulus, which is promising for dental applications.

The reliability of all ceramic materials was evaluated at clinically relevant stress levels, as per ISO 6872:2015 requirements (International-Standard-Organization, 2015). ZTA composite presented higher probability of survival than Al_2O_3 at 300 MPa, and 3Y-TZP outperformed ZTA and Al_2O_3, at a stress level compatible to the indication of 3-unit anterior fixed dental prostheses (FDPs), with no significant influence of aging. Al_2O_3-based materials (including ZTA) reliability dropped significantly at missions higher than 500 MPa, which still discourage its indication for the manufacture of FDP infrastructures of three or more units at posterior regions. Although ZTA composites appears to present an interesting microstructure, aging resistance, and strength, improvements in the composition, synthesis, and/or processing methods are still required to achieve higher reliability and increase the potential application for long-span prostheses. Also, clinical studies are required to evaluate the performance of ZTA-based prosthesis.

5. Conclusion

Aging did not affect either the crystalline content and microstructure nor the fatigue performance of ZTA and Al_2O_3, while second-generation 3Y-TZP evidenced a significant increase in the monoclinic content and characteristic strength after aging and/or fatigue.

CRediT authorship contribution statement

Ernesto B. Benalcázar Jalkh: Writing – review & editing, Writing – original draft, Validation, Software, Methodology, Investigation, Formal analysis, Conceptualization. **Edmara T.P. Bergamo:** Writing – review & editing, Validation, Software, Methodology, Investigation, Formal analysis, Conceptualization. **Tiago M.B. Campos:** Writing – review & editing, Visualization, Software, Resources, Investigation, Formal analysis. **Everardo N.S. de Araújo-Júnior:** Visualization, Validation, Software, Methodology, Investigation, Formal analysis, Data curation. **Adolfo C.O. Lopes:** Visualization, Validation, Software, Methodology, Investigation, Formal analysis, Data curation. **Sérgio M. Tebcherani:** Writing – review & editing, Visualization, Validation, Supervision. **Satoshi Yamaguchi:** Writing – review & editing, Visualization, Validation, Supervision. **Luis A. Genova:** Supervision, Resources, Methodology, Investigation, Conceptualization. **Petra C. Gierthmuehlen:** Writing – review & editing, Visualization, Validation. **Lukasz Witek:** Writing – review & editing, Visualization, Validation, Supervision, Formal analysis. **Paulo G. Coelho:** Writing – review & editing, Validation, Supervision, Resources. **Estevam A. Bonfante:** Writing – review & editing, Validation, Supervision, Resources, Project administration, Methodology, Funding acquisition, Conceptualization.

Declaration of competing interest

The authors declare that they have no known competing financial interests or personal relationships that could have appeared to influence the work reported in this paper.

Data availability

Data will be made available on request.

Acknowledgments

This work was supported by São Paulo Reuter Foundation (FAPESP), grant # 2012/19078-7, 2021/06730-7, EMU 2016/18818-8, and scholarships # 2022/07157-1; 2018/03072-6; 2019/00452-5; 2019/08693-1 and BEPE 2021/08018-2; 2016/17793-1 and 2017/19362-0. By Conselho Nacional de Desenvolvimento Científico e Tecnológico (CNPq), Grant # 307255/2021-2. By CAPES Financial Code 001.

References

Abernethy, R.B., Breneman, J., Medlin, C., Reinman, G.L., 1983. Weibull Analysis Handbook. Pratt and Whitney West Palm beach fl Government Products DIV.
Al-Hajjar, M., Gremillard, L., Begand, S., Oberbach, T., Hans, K., Delfosse, D., Chevalier, J., Jennings, L.M., 2019. Combined wear and ageing of ceramic-on-ceramic bearings in total hip replacement under edge loading conditions. J. Mech. Behav. Biomed. Mater. 98, 40–47.
Becher, P.F., Swain, M.V., 1992. Grain-size-dependent transformation behavior in polycrystalline tetragonal zirconia. J. Am. Ceram. Soc. 75 (3), 493–502.
Benalcazar Jalkh, E.B., Bergamo, E.T.P., Monteiro, K.N., Cesar, P.F., Genova, L.A., Lopes, A.C.O., Lisboa Filho, P.N., Coelho, P.G., Santos, C.F., Bortolin, F., Piza, M.M. T., Bonfante, E.A., 2020a. Aging resistance of an experimental zirconia-toughened alumina composite for large span dental prostheses: optical and mechanical characterization. J. Mech. Behav. Biomed. Mater. 104, 103659.
Benalcazar Jalkh, E.B., Monteiro, K.N., Cesar, P.F., Genova, L.A., Bergamo, E.T.P., Lopes, A.C.O., Lima, E., Lisboa-Filho, P.N., Campos, T.M.B., Witek, L., Coelho, P.G., Borges, A.F.S., Bonfante, E.A., 2020b. Aging resistant ZTA composite for dental applications: microstructural, optical and mechanical characterization. Dent. Mater. 36 (9), 1190–1200.
Bonfante, E.A., Coelho, P.G., 2016. A critical perspective on mechanical testing of implants and prostheses. Adv. Dent. Res. 28 (1), 18–27.
Chevalier, J., 2006. What future for zirconia as a biomaterial? Biomaterials 27 (4), 535–543.
Chevalier, J., Cales, B., Drouin, J.M., 1999. Low-temperature aging of Y-TZP ceramics. J. Am. Ceram. Soc. 82 (8), 2150–2154.
Chevalier, J., De Aza, A.H., Fantozzi, G., Schehl, M., Torrecillas, R., 2000. Extending the lifetime of ceramic orthopaedic implants. Adv. Mater. 12 (21), 1619–1621.
Chevalier, J., Grandjean, S., Kuntz, M., Pezzotti, G., 2009a. On the kinetics and impact of tetragonal to monoclinic transformation in an alumina/zirconia composite for arthroplasty applications. Biomaterials 30 (29), 5279–5282.
Chevalier, J., Gremillard, L., 2009. Ceramics for medical applications: a picture for the next 20 years. J. Eur. Ceram. Soc. 29 (7), 1245–1255.
Chevalier, J., Gremillard, L., Deville, S., 2007a. Low-temperature degradation of Zirconia and implications for biomedical implants. Annu. Rev. Mater. Res. 37, 1–32.
Chevalier, J., Gremillard, L., Deville, S., 2007b. Low-temperature degradation of zirconia and implications for biomedical implants. Annu. Rev. Mater. Res. 37, 1–32.

Chevalier, J., Gremillard, L., Virkar, A.V., Clarke, D.R., 2009b. The tetragonal-monoclinic transformation in zirconia: lessons learned and future trends. J. Am. Ceram. Soc. 92 (9), 1901–1920.
Chevalier, J., Gremillard, L., Virkar, A.V., Clarke, D.R., 2009c. The tetragonal-monoclinic transformation in zirconia: lessons learned and future trends. J. Am. Ceram. Soc. 92 (9), 1901–1920.
Cotic, J., Kocjan, A., Panchevska, S., Kosmac, T., Jevnikar, P., 2021. In vivo ageing of zirconia dental ceramics - Part II: highly-translucent and rapid-sintered 3Y-TZP. Dent. Mater. 37 (3), 454–463.
Garvie, R.C.H., Pascoe, R.H., T, R., 1975. Ceramic steel. Nature 258, 703–704.
Howard, D.P., Wall, P.D.H., Fernandez, M.A., Parsons, H., Howard, P.W., 2017. Ceramic-on-ceramic bearing fractures in total hip arthroplasty: an analysis of data from the National Joint Registry. Bone Joint Lett. J 99-B (8), 1012–1019.
International-Standard-Organization, 2015a. International Standard ISO 6872: Dentistry-Ceramic Materials. ISO.
International-Standard-Organization, 2015b. ISO 13356:2015 Implants for Surgery — Ceramic Materials Based on Yttria-Stabilized Tetragonal Zirconia (Y-TZP).
Joda, T., Zarone, F., Ferrari, M., 2017. The complete digital workflow in fixed prosthodontics: a systematic review. BMC Oral Health 17 (1), 124.
Jung, R.E., Holderegger, C., Sailer, I., Khraisat, A., Suter, A., Hammerle, C.H., 2008. The effect of all-ceramic and porcelain-fused-to-metal restorations on marginal peri-implant soft tissue color: a randomized controlled clinical trial. Int. J. Periodontics Restor. Dent. 28 (4), 357–365.
Kim, H.-T., Han, J.-S., Yang, J.-H., Lee, J.-B., Kim, S.-H., 2009a. The effect of low temperature aging on the mechanical property & phase stability of Y-TZP ceramics. J. Adv. Prosthodont. 1 (3), 113–117.
Kim, H.K., Kim, S.H., 2018. Effect of hydrothermal aging on the optical properties of precolored dental monolithic zirconia ceramics. J. Prosthet. Dent 121 (4), 676–682.
Kim, H.T., Han, J.S., Yang, J.H., Lee, J.B., Kim, S.H., 2009b. The effect of low temperature aging on the mechanical property & phase stability of Y-TZP ceramics. J. Adv. Prosthodont. 1 (3), 113–117.
Kocjan, A., Cotic, J., Kosmac, T., Jevnikar, P., 2020. In vivo aging of zirconia dental ceramics - Part I: biomedical grade 3Y-TZP. Dent. Mater. 37 (3), 443–453.
Koenig, V., Bekaert, S., Dupont, N., Vanheusden, A., Le Goff, S., Douillard, T., Chevalier, J., Djaker, N., Lamy de la Chapelle, M., Amiard, F., Dardenne, N., Wulfman, C., Mainjot, A., 2021. Intraoral low-temperature degradation of monolithic zirconia dental prostheses: results of a prospective clinical study with ex vivo monitoring. Dent. Mater. 37 (7), 1134–1149.
Kurtz, S.M., Kocagoz, S., Arnholt, C., Huet, R., Ueno, M., Walter, W.L., 2014. Advances in zirconia toughened alumina biomaterials for total joint replacement. J. Mech. Behav. Biomed. Mater. 31, 107–116.
Lopes, A.C.O., Coelho, P.G., Witek, L., Benalcazar Jalkh, E.B., Genova, L.A., Monteiro, K. N., Cesar, P.F., Lisboa-Filho, P.N., Bergamo, E.T.P., Ramalho, I.S., Campos, T.M.B., Bonfante, E.A., 2020. Microstructural, mechanical, and optical characterization of an experimental aging-resistant zirconia-toughened alumina (ZTA) composite. Dent. Mater. 36 (12), e365–e374.
Lopes, A.C.O., Coelho, P.G., Witek, L., Jalkh, E.B.B., Gênova, L.A., Monteiro, K.N., Cesar, P.F., Lisboa Filho, P.N., Bergamo, E.T.P., Ramalho, I.S., 2019. Nanomechanical and microstructural characterization of a zirconia-toughened alumina composite after aging. Ceram. Int. 45 (7), 8840–8846.
Lucas, T.J., Lawson, N.C., Janowski, G.M., Burgess, J.O., 2015. Effect of grain size on the monoclinic transformation, hardness, roughness, and modulus of aged partially stabilized zirconia. Dent. Mater. 31 (12), 1487–1492.
Nelson, W., 2004. Accelerated Testing: Statistical Models, Test Plans and Data Analysis. John Wiley & Sons, New York.
Pereira, G.K., Venturini, A.B., Silvestri, T., Dapieve, K.S., Montagner, A.F., Soares, F.Z., Valandro, L.F., 2015. Low-temperature degradation of Y-TZP ceramics: a systematic review and meta-analysis. J. Mech. Behav. Biomed. Mater. 55, 151–163.
Perrichon, A., Liu, B.H., Chevalier, J., Gremillard, L., Reynard, B., Farizon, F., Liao, J.D., Geringer, J., 2017. Ageing, shocks and wear mechanisms in ZTA and the long-term performance of hip joint materials. Materials 10 (6).
Piconi, C., Maccauro, G., Pilloni, L., Burger, W., Muratori, F., Richter, H.G., 2006. On the fracture of a zirconia ball head. J. Mater. Sci. Mater. Med. 17 (3), 289–300.
Pjetursson, B.E., Fehmer, V., Sailer, I., 2022. EAO position paper: material selection for implant-supported restorations. Int. J. Prosthodont. (IJP) 35 (1), 7–16.
Pjetursson, B.E., Sailer, I., Makarov, N.A., Zwahlen, M., Thoma, D.S., 2017. Corrigendum to "All-ceramic or metal-ceramic tooth-supported fixed dental prostheses (FDPs)? A systematic review of the survival and complication rates. Part II: multiple-unit FDPs. Dent. Mater. 31 (6), 624–639, 2015, Dent Mater 33(1): e48-e51.
Pjetursson, B.E., Valente, N.A., Strasding, M., Zwahlen, M., Liu, S., Sailer, I., 2018. A systematic review of the survival and complication rates of zirconia-ceramic and metal-ceramic single crowns. Clin. Oral Implants Res. 29 (Suppl. 16), 199–214.
Prado, P., Monteiro, J.B., Campos, T.M.B., Thim, G.P., de Melo, R.M., 2019. Degradation kinetics of high-translucency dental zirconias: mechanical properties and in-depth analysis of phase transformation. J. Mech. Behav. Biomed. Mater. 102, 103482.
Rondinella, A., Marin, E., Boschetto, F., Zanocco, M., Zhu, W., Affatato, S., Yamamoto, K., Tateiwa, T., Pezzotti, G., 2018. Degradation phenomena occurring in the conical taper of a short-term retrieved ZTA femoral head: a case study. Mater. Des. 157, 362–370.
Sailer, I., Balmer, M., Husler, J., Hammerle, C.H.F., Kanel, S., Thoma, D.S., 2018a. 10-year randomized trial (RCT) of zirconia-ceramic and metal-ceramic fixed dental prostheses. J. Dent. 76, 32–39.
Sailer, I., Makarov, N.A., Thoma, D.S., Zwahlen, M., Pjetursson, B.E., 2015. All-ceramic or metal-ceramic tooth-supported fixed dental prostheses (FDPs)? A systematic review of the survival and complication rates. Part I: single crowns (SCs). Dent. Mater. 31 (6), 603–623.
Sailer, I., Makarov, N.A., Thoma, D.S., Zwahlen, M., Pjetursson, B.E., 2016. Corrigendum to "All-ceramic or metal-ceramic tooth- supported fixed dental prostheses (FDPs)? A systematic review of the survival and complication rates. Part I: single crowns (SCs). Dent. Mater. 31 (6), 603–623, 2015, Dent Mater 32(12): e389-e390.
Sailer, I., Strasding, M., Valente, N.A., Zwahlen, M., Liu, S., Pjetursson, B.E., 2018b. A systematic review of the survival and complication rates of zirconia-ceramic and metal-ceramic multiple-unit fixed dental prostheses. Clin. Oral Implants Res. 29 (Suppl. 16), 184–198.
Stump, D.M., Budiansky, B., 1989. Crack-growth resistance in transformation-toughened ceramics. Int. J. Solid Struct. 25 (6), 635–646.
Tong, H., Tanaka, C.B., Kaizer, M.R., Zhang, Y., 2016. Characterization of three commercial Y-TZP ceramics produced for their High-Translucency, High-Strength and High-Surface Area. Ceram. Int. 42 (1), 1077–1085.
Toraya, H., Yoshimura, M., Somiya, S., 1984. Calibration curve for quantitative-analysis of the monoclinic-tetragonal Zro2 system by X-ray-diffraction. J. Am. Ceram. Soc. 67 (6), C119–C121.
Walton, T.R., 2013. The up to 25-year survival and clinical performance of 2,340 high gold-based metal-ceramic single crowns. Int. J. Prosthodont. (IJP) 26 (2), 151–160.
Zhang, Y., Lawn, B.R., 2017. Novel zirconia materials in dentistry. J. Dent. Res., 22034517737483
Zhao, W., Elsayed, E.A., 2005. A general accelerated life model for step-stress testing. IIE Trans. 37 (11), 1059–1069.